

Contribution from the Fachbereich Chemie, Bergische Universität Wuppertal—Gesamthochschule, D-5600 Wuppertal 1, Germany, and Polyatomics Research Institute, 1101 San Antonio Road, Mountain View, California 94043

Ab Initio Calculation of Harmonic Force Fields and Vibrational Spectra of the Fluoroarsines $\text{AsH}_n\text{F}_{3-n}$ ($n = 0-3$) and the Fluoroarsoranones $\text{AsH}_n\text{F}_{5-n}$ ($n = 0-5$)

Jürgen Breidung,[†] Walter Thiel,^{*,†} and Andrew Komornicki[‡]

Received April 23, 1990

Ab initio self-consistent-field calculations using effective core potentials and polarized double- ζ basis sets are reported for the title compounds and the analogous phosphorus compounds. The most stable trigonal-bipyramidal isomers of the fluoroarsoranones are those with the maximum number of axial fluorine atoms, as in the case of the fluorophosphoranones. For the known molecules AsH_3 , AsF_3 , and AsF_5 , the calculated geometries and vibrational frequencies agree well with the experimental data, and improvements to the current empirical force field of AsF_5 are suggested. Predictions are made for the vibrational spectra of the other molecules, which are unknown, and plots of the calculated gas-phase infrared spectra at 300 K are presented for AsH_5 , AsH_4F , and AsH_3F_2 , as an aid to their spectroscopic identification. Trends in the calculated properties of the fluoroarsoranones are discussed and found to be very similar to those for the fluorophosphoranones.

Introduction

The harmonic force fields and vibrational spectra of the fluorophosphines $\text{PH}_n\text{F}_{3-n}$ ($n = 0-3$) and fluorophosphoranones $\text{PH}_n\text{F}_{5-n}$ ($n = 0-5$) have recently been studied at the ab initio level.^{1,2} This work has provided predictions of the gas-phase infrared spectra of PH_2F , PH_4F , and PH_5 , revised or extended assignments for PHF_4 , PH_2F_3 , and PH_3F_2 , and improved force fields for PHF_2 , PF_3 , and PF_5 .

The present paper reports analogous calculations for the fluoroarsines $\text{AsH}_n\text{F}_{3-n}$ ($n = 0-3$) and fluoroarsoranones $\text{AsH}_n\text{F}_{5-n}$ ($n = 0-5$). Experimentally, gas-phase rotational and vibrational spectra are available only for AsH_3 ,³⁻¹¹ AsF_3 ,¹²⁻¹⁵ and AsF_5 ,¹⁶⁻¹⁸ since the other fluoroarsines and fluoroarsoranones are still unknown. Empirical force fields have been derived from the experimental data for AsH_3 ,^{11,19} AsF_3 ,^{15,20,21} and AsF_5 .^{16,22,23} There have been several ab initio studies of AsH_3 and AsF_3 ,²⁴⁻²⁸ which were mainly concerned with their structures and inversion barriers. Very recently, the harmonic force fields and vibrational spectra of these two molecules have been calculated at the ab initio level.²⁹ In the series of the fluoroarsoranones, only AsH_5 ,²⁶ and AsF_5 ³⁰ have been the subject of ab initio work, which dealt with their structures and the barrier for the Berry pseudorotation process.³¹

In view of this situation, the present paper provides a number of theoretical predictions for the fluoroarsines and fluoroarsoranones, especially with regard to their gas-phase vibrational spectra. The calculated geometries, frequencies, force constants, and other properties are studied to identify systematic trends in the series of the fluoroarsoranones and to compare them with those for the fluorophosphoranones.

Details of the Calculations

All quantum-chemical calculations were carried out at the Hartree-Fock level by using the GRADSCF program system,³² which was modified to handle analytical second derivatives for effective core potentials (ECP).³³ Standard ECPs for P and As were taken from the literature,³⁴ and the corresponding ECP basis sets³⁴ were used in a double- ζ contraction [3/21] augmented by one set of six polarization d functions with the following exponents: P, 0.55; As, 0.35. The standard 6-31G** basis^{35,36} was employed for H and F.

Molecular geometries were completely optimized within the constraint of a given point group symmetry, which was chosen to be C_{3v} (AsH_3 , AsF_3) or C_4 (AsH_2F , AsHF_2) in the case of the fluoroarsines. The fluoroarsoranones were always treated as trigonal bipyramids. Their most stable isomers have the maximum number of fluorine substituents in axial positions (see next section), so that in these cases the point group symmetries were D_{3h} (AsH_5 , AsH_3F_2 , AsF_5), C_{3v} (AsH_4F), and C_{2v} (AsH_2F_3 , AsHF_4). The point group symmetries of the less stable isomers of the arsanones are specified in the next section. The Cartesian force constants and Cartesian dipole moment derivatives were evaluated analytically at the theoretical equilibrium geometries and then converted to spectroscopic constants in the usual manner.³⁷⁻³⁹

The conventions for defining the internal and symmetry coordinates in the fluoroarsines and fluoroarsoranones were the same as before.^{1,2} In-

- Breidung, J.; Thiel, W. *J. Phys. Chem.* **1988**, *92*, 5597.
- Breidung, J.; Thiel, W.; Komornicki, A. *J. Phys. Chem.* **1988**, *92*, 5603.
- Sarka, K.; Papousek, D.; Rao, K. N. *J. Mol. Spectrosc.* **1971**, *37*, 1.
- Chu, F. Y.; Oka, T. *J. Chem. Phys.* **1974**, *60*, 4612.
- Olson, W. B.; Maki, A. G.; Sams, R. L. *J. Mol. Spectrosc.* **1975**, *55*, 252.
- Helms, D. A.; Gordy, W. *J. Mol. Spectrosc.* **1978**, *69*, 473.
- Burenin, A. V.; Kazakov, V. P.; Krupnov, A. F.; Mel'nikov, A. A.; Shapin, S. M. *J. Mol. Spectrosc.* **1982**, *94*, 253.
- Carloti, M.; Di Lonardo, G.; Fusina, L. *J. Mol. Spectrosc.* **1983**, *102*, 310.
- Di Lonardo, G.; Fusina, L.; Johns, J. W. C. *J. Mol. Spectrosc.* **1984**, *104*, 282.
- Kazakov, V. P.; Krupnov, A. F.; Saveliev, V. N.; Ulenikov, O. N. *J. Mol. Spectrosc.* **1987**, *123*, 340.
- McRae, G. A.; Gerry, M. C. L.; Wong, M.; Ozier, I.; Cohen, E. A. *J. Mol. Spectrosc.* **1987**, *123*, 321.
- Hoskins, L. C.; Lord, R. C. *J. Chem. Phys.* **1965**, *43*, 155.
- Reichman, S.; Overend, J. *Spectrochim. Acta* **1970**, *26A*, 379.
- Chikaraishi, T.; Hirota, E. *Bull. Chem. Soc. Jpn.* **1973**, *46*, 2314.
- Smith, J. G. *Mol. Phys.* **1978**, *35*, 461.
- Hoskins, L. C.; Lord, R. C. *J. Chem. Phys.* **1967**, *46*, 2402.
- Selig, H.; Holloway, J. H.; Tyson, J.; Claassen, H. H. *J. Chem. Phys.* **1970**, *53*, 2559.
- Bernstein, L. S.; Abramowitz, S.; Levin, I. W. *J. Chem. Phys.* **1976**, *64*, 3228.
- Duncan, J. L. *J. Mol. Spectrosc.* **1976**, *60*, 225.
- Mirri, A. M. *J. Chem. Phys.* **1967**, *47*, 2823.
- Konaka, S. *Bull. Chem. Soc. Jpn.* **1970**, *43*, 3107.
- Levin, I. W. *J. Mol. Spectrosc.* **1970**, *33*, 61.
- Hoskins, L. C.; Perng, C. N. *J. Chem. Phys.* **1971**, *55*, 5063.
- Marynick, D. S. *Chem. Phys. Lett.* **1980**, *71*, 101.
- Marynick, D. S.; Rosen, D. C.; Liebman, J. F. *J. Mol. Struct.* **1983**, *94*, 47.
- Trinquier, G.; Daudey, J.-P.; Caruana, G.; Madaule, Y. *J. Am. Chem. Soc.* **1984**, *106*, 4794.
- Dixon, D. A.; Arduengo, A. J. *J. Am. Chem. Soc.* **1987**, *109*, 338.
- Clotet, A.; Rubio, J.; Illas, F. *J. Mol. Struct.* **1988**, *164*, 351.
- Schneider, W.; Thiel, W.; Komornicki, A. *J. Phys. Chem.* **1990**, *94*, 2810.
- Dobbs, K. D.; Hehre, W. J. *J. Comput. Chem.* **1986**, *7*, 359.
- Berry, R. S. *J. Chem. Phys.* **1960**, *32*, 933.
- Komornicki, A. *GRADSCF: An ab Initio Gradient Program System, Version 9.5*; Polyatomics Research Institute: Mountain View, CA, 1988.
- Breidung, J.; Thiel, W.; Komornicki, A. *Chem. Phys. Lett.* **1988**, *153*, 76.
- Wadt, W. R.; Hay, P. J. *J. Chem. Phys.* **1985**, *82*, 284.
- Hehre, W. J.; Ditchfield, R.; Pople, J. A. *J. Chem. Phys.* **1972**, *56*, 2257.

[†] Bergische Universität Wuppertal.

[‡] Polyatomics Research Institute.

Table I. Molecular Geometries of the Fluoroarsines^a

molecule	type ^b	r_e , Å	R_e , Å	α_e , deg	β_e , deg	γ_e , deg	ref
AsH ₃	T	1.509		94.3			
	E	1.5111		92.07			8
	E	1.513 (2)		92.08 (7)			11
AsH ₂ F	T	1.514	1.721	93.0		96.7	
AsHF ₂	T	1.520	1.701		96.9	95.1	
AsF ₃	T		1.683		95.7		
	E		1.7041 (10)		95.77 (12)		15

^a For notation see text. ^b T = theoretical; E = experimental; uncertainty of last digit given in parentheses.

ternal coordinates: r , an As–H distance; R , an As–F distance; α , a HAsH angle; β , a FAsF angle; γ , a HAsF angle. The symmetry coordinates S_i for the fluoroarsines were defined as usual^{40–42} (see Tables I and II of ref 1). The definitions for the fluoroarsoranones were the same as in ref 2 (see Tables I–III therein), in agreement with the usual conventions.^{16,22,43} For scaling the theoretical harmonic force fields in symmetry coordinates, we employed the same procedure⁴⁴ as in our previous studies.^{1,2,39} A scale factor c_i was introduced for each diagonal force constant F_{ii} associated with symmetry coordinate S_i . The scaled off-diagonal force constants were then given in terms of the unscaled ones by $F_{ij}^s = c_i^{1/2} F_{ij} c_j^{1/2}$. Since identical scale factors apply for qualitatively similar distortions, there are altogether five independent scale factors (i.e., c_r , c_R , c_α , c_β , and c_γ), for the five types of internal coordinates listed above. The detailed assignment of these scale factors c_i to symmetry coordinates S_i is shown in Tables I and II of ref 1 and in Tables I–III of ref 2, respectively. The optimum values for c_r , c_R , c_α , and c_β were obtained³⁹ by minimizing the root-mean-square (rms) deviation between the frequencies ν_i calculated from the scaled theoretical force field and the observed fundamental frequencies ν_i^{obsd} of AsH₃ and AsF₃, respectively. The optimum value for c_γ was approximated as the mean value of c_α and c_β . These optimum scale factors were transferred to all other As-containing molecules considered in this study.

Results and Discussion

In this section we present our theoretical results, first for the fluoroarsines AsH_nF_{3–n} ($n = 0–3$) and then for the fluoroarsoranones AsH_nF_{5–n} ($n = 0–5$). These results are compared with experimental data, if available, and serve as predictions otherwise. In addition, we discuss the trends in the calculated properties of the fluoroarsoranones upon successive fluorine substitution and compare them with those of the fluorophosphoranones. In these comparisons we refer both to previous all-electron ab initio results for the fluorophosphoranones^{1,2} and to new valence-electron ECP results. In agreement with previous experience,³⁹ the new valence-electron ECP results for the phosphorus compounds are generally very similar to the corresponding all-electron results,^{1,2} the deviations being e.g. less than 0.002 Å for the P–H bond lengths, 0.005 ± 0.003 Å for the P–F bond lengths, and 5–13 cm⁻¹ (rms) for the unscaled theoretical frequencies of the fluorophosphoranones. Therefore we report the new ECP results for the phosphorus compounds⁴⁶ only if directly needed in comparisons with the arsenic compounds.

Table I lists the calculated and observed^{8,11,15} molecular geometries of the fluoroarsines. The theoretical results for AsH₃ and AsF₃ agree well with experiment and are similar in accuracy to those for the corresponding phosphines.¹ The theoretical predictions for AsH₂F and AsHF₂ are therefore also expected to be realistic. Upon successive fluorine substitution, there is a pronounced shortening of the As–F bond length, while the As–H bond length increases only slightly. Similar trends are found for

Table II. Vibrational Frequencies ω_i and ν_i (cm⁻¹) and Infrared Intensities A_i (km/mol) for the Fluoroarsines

molecule	mode	description ^a	calcd ^b			obsd ^c	
			ω_i	ν_i	A_i	ν_i^{obsd}	ref
AsH ₃	a ₁	ν_1 As–H s-str	2347	2119	56	2115.17	5
		ν_2 HAsH s-def	1025	906	39	906.75	9, 10
	e	ν_3 As–H d-str	2354	2125	301	2126.42	5
		ν_4 HAsH d-def	1130	999	39	999.22	9, 10
AsH ₂ F	a'	ν_1 As–H s-str	2327	2100	113		
		ν_2 HAsH sciss	1122	992	37		
	a''	ν_3 HAsF s-bend	926	826	33		
		ν_4 As–F str	734	673	102		
		ν_5 As–H a-str	2334	2106	199		
		ν_6 HAsF a-bend	870	775	11		
AsHF ₂	a'	ν_1 As–H str	2309	2084	200		
		ν_2 HAsF s-bend	948	846	53		
	a''	ν_3 As–F s-str	768	704	94		
		ν_4 FAsF sciss	295	266	14		
AsF ₃	a ₁	ν_1 As–F s-str	748	686	132		
		ν_2 FAsF s-def	807	740	82	740.55 s	13
	e	ν_3 As–F d-str	380	342	41	336.5 m	12
		ν_4 FAsF d-def	766	703	273	702.2 s	12

^a Based on the calculated potential energy distributions. ^b For scale factors see Table III; intensities refer to the scaled theoretical force fields; i.e., the original ab initio Cartesian dipole moment derivatives are used with the modified (scaled) normal-mode eigenvectors to determine the intensities. ^c Infrared frequencies and relative intensities in standard notation.

Table III. Scale Factors c_i and Rms Deviations σ (cm⁻¹)

molecule	c_r	c_R	c_α	c_β	c_γ	σ
AsH ₃	0.8147		0.7819			1.8
AsF ₃		0.8418		0.8084		2.8
std ^a	0.8147	0.8418	0.7819	0.8084	0.7952 ^b	

^a Used for AsH₂F, AsHF₂, and AsH_nF_{5–n} ($n = 0–5$). ^b Mean value of c_α and c_β ; see text.

the fluorophosphines¹ and the fluoroamines,⁴⁵ with shifts of similar magnitude. Like PH₂F,¹ AsH₂F is predicted to behave as a nearly prolate symmetric-top molecule, since its rotational constants B_c and C_c differ by less than 1%.⁴⁶

Table II contains the unscaled theoretical harmonic frequencies ω_i , the scaled theoretical frequencies ν_i , and the calculated infrared intensities A_i , together with the available experimental data for AsH₃^{5,9,10} and AsF₃.^{12,13} The corresponding scale factors and the rms deviations between the scaled theoretical and observed frequencies are collected in Table III. The optimized scale factors c_r and c_α for AsH₃ and c_R and c_β for AsF₃ form the set of our standard scale factors, together with the scale factor c_γ for the HAsF bending coordinates in AsH₂F and AsHF₂. Due to the lack of suitable reference data, this factor has been set to $c_\gamma = (c_\alpha + c_\beta)/2$, which seems to be justified by the similarity of c_α and c_β (see Table III and supplementary material).

The scaled theoretical frequencies for AsH₃ and AsF₃ are in excellent agreement with the observed frequencies, for reasons discussed before.²⁹ According to previous experience,^{1,2,39,47} the

- (36) Hariharan, P. C.; Pople, J. A. *Theor. Chim. Acta* 1973, 28, 213.
 (37) Wilson, E. B., Jr.; Decius, J. C.; Cross, P. C. *Molecular Vibrations*; McGraw-Hill: New York, 1955.
 (38) Califano, S. *Vibrational States*; Wiley: New York, 1976.
 (39) Schneider, W.; Thiel, W. *J. Chem. Phys.* 1987, 86, 923.
 (40) Duncan, J. L.; Mills, I. M. *Spectrochim. Acta* 1964, 20, 523.
 (41) Durig, J. R.; Zozulin, A. J.; Odom, J. D.; Streusand, B. J. *J. Raman Spectrosc.* 1979, 8, 259.
 (42) Dunning, V. D.; Taylor, R. C. *Spectrochim. Acta* 1979, 35A, 479.
 (43) Shimanouchi, T. *J. Phys. Chem. Ref. Data* 1977, 6, 993.
 (44) Pulay, P.; Fogarasi, G.; Pongor, G.; Boggs, J. E.; Vargha, A. *J. Am. Chem. Soc.* 1983, 105, 7037.
 (45) Christen, D.; Minkwitz, R.; Nass, R. *J. Am. Chem. Soc.* 1987, 109, 7020.
 (46) Breidung, J. Doctoral Thesis, University of Wuppertal, 1989.

- (47) Schneider, W.; Thiel, W.; Komornicki, A. *J. Phys. Chem.* 1988, 92, 5611.

Table IV. Relative Energies ΔE_M (kcal/mol) of the Trigonal-Bipyramidal Isomers of the Fluoroarsoranes ($M = \text{As}$) and the Fluorophosphoranes ($M = \text{P}$)

molecule	isomer ^a	symm	ΔE_{As}	ΔE_P^b	N_{im}^c
MH ₄ F	B	C _{3v}	0.00	0.00	0
	C	C _{2v}	11.57	10.69 (15.95)	1
MH ₃ F ₂	A	D _{3h}	0.00	0.00	0
	B	C _s	14.29	12.39 (13.61)	0
	C	C _{2v}	23.95 ^d	20.26 ^d (21.03)	0
MH ₂ F ₃	A	C _{2v}	0.00	0.00	0
	B	C _s	12.90 ^d	9.65 (10.73)	0 ^e
	C	D _{3h}	10.90	9.59 (9.71)	0
MHF ₄	A	C _{2v}	0.00	0.00	0
	B	C _{3v}	5.66	5.69 (5.82)	0

^aA, B, C with 2, 1, 0 axial fluorine atoms. ^bValues in parentheses from ref 58 (6-31G* basis; only bond lengths have been optimized). ^cNumber of imaginary vibrational frequencies. ^dThese values do not refer to a completely optimized geometry, but only to bond lengths optimized by using fixed bond angles of an ideal trigonal bipyramid; see text. If, alternatively, the equatorial bond angles are held fixed at the optimized values for a planar MHF₂ molecule, we obtain the following for ΔE_M (kcal/mol): AsH₃F₂, 26.66; PH₃F₂, 22.15; AsH₂F₃, 14.13. ^eThis entry refers only to $M = \text{P}$.

transfer of scale factors between related molecules is usually accompanied by errors of typically 20 cm⁻¹ in the scaled theoretical frequencies. Therefore we expect errors of this magnitude in the scaled theoretical frequencies of AsH₂F and AsHF₂. Judging from the results for the fluorophosphines,¹ the absolute infrared intensities of the vibrational transitions in the fluoroarsines may well be overestimated by the theoretical values in Table II, but we are confident that the relative intensities are predicted reliably.

The scaled theoretical force fields of the fluoroarsines are given in the supplementary material. Those for AsH₃ and AsF₃ have been discussed recently²⁹ and were found to agree well with the most recent empirical force fields.^{11,15}

Table IV contains the calculated relative energies ΔE_M of the trigonal-bipyramidal (tbp) isomers of the fluoroarsoranes ($M = \text{As}$). Table IV also contains the corresponding data for the analogous fluorophosphoranes ($M = \text{P}$), for the sake of comparison. In the case of MH₃F₂ and MH₂F₃ three tbp isomers are possible: isomer A with two axial fluorine atoms, isomer B with only one axial fluorine atom, and isomer C with none. On the basis of this notation, MH₄F can have isomers B and C, and MHF₄ isomers A and B. The geometries of all isomers were completely optimized within the constraint of the given point group symmetry (see Table IV). These optimizations were usually successful. However, for isomers C of MH₃F₂ ($M = \text{P}, \text{As}$) and isomer B of AsH₂F₃, complete optimizations yielded structures of type A instead of types C and B, respectively. Therefore we fixed the bond angles to the values of an ideal trigonal bipyramid and optimized only the bond lengths in these exceptional cases, so that the corresponding relative energies (see Table IV) do not refer to stationary points. As one can see from the last column of Table IV, the other optimized structures usually correspond to local minima with no negative eigenvalues (i.e., no imaginary frequencies) of the associated force constant matrices, with the exception of isomer C of MH₄F ($M = \text{P}, \text{As}$), which is a transition state with one imaginary b₁ frequency (252i cm⁻¹ for $M = \text{P}$; 287i cm⁻¹ for $M = \text{As}$) and a b₁ transition vector leading directly to isomer B.

The relative energies of the different tbp isomers (see Table IV) show that the fluoroarsoranes behave like the fluorophosphoranes both qualitatively and quantitatively: a trigonal bipyramid with the maximum number of fluorine substituents in axial positions leads to the most stable tbp isomer in each case, a property that is well-known for the fluorophosphoranes;⁴⁸⁻⁵⁸

furthermore the relative isomer energies are very similar for both series of molecules. Our calculated relative energies for the isomers of the fluorophosphoranes may be compared with recent values⁵⁸ obtained with the all-electron 6-31G* basis set by optimization of bond lengths only (see Table IV, values in parentheses). The two sets of theoretical data agree very well, the only noticeable difference being associated with isomer C of PH₄F, which is now known to be an activated complex (see above) rather than a local minimum.

Table V lists the molecular geometries of the different tbp isomers of the fluoroarsoranes. For the purpose of comparisons, we have also included the corresponding results for the fluorophosphoranes. Inspecting the most stable isomers first, one sees that equatorial bonds are always calculated to be considerably shorter than axial bonds of the same kind, and As-H as well as As-F bond lengths decrease with increasing fluorine substitution. The fluorophosphoranes show the same trend² (see also Table V). For the known fluorophosphoranes PH_nF_{5-n} ($n = 0-3$) the theoretical and experimental⁵⁹⁻⁶² structural data may be compared. The weighted averages for the P-F distances agree well (PH₃F₂, 1.633 vs 1.647 Å experimentally;⁵⁹ PH₂F₃, 1.587 vs 1.592 and 1.590 Å, respectively;^{60,61} PHF₄, 1.562 vs 1.568 and 1.564 Å, respectively;^{60,61} PF₅, 1.545 vs 1.548 Å⁶²), but the calculations always underestimate the differences between the axial and equatorial bond lengths (PH₂F₃, 0.057 vs 0.079 and 0.069 Å, respectively;^{60,61} PHF₄, 0.047 vs 0.057 and 0.054 Å, respectively;^{60,61} PF₅, 0.035 vs 0.047 Å experimentally⁶²). The calculated P-H bond lengths are close to the experimental r_o ⁵⁹ and r_z ⁶⁰ values, whereas the published r_a distances⁶¹ appear to be too short. The agreement for the bond angles in PH₂F₃ and PHF₄ is as good as can be expected.⁶³ For AsF₅, the calculation underestimates both the weighted average for the As-F distances (1.655 vs 1.678 Å experimentally⁶⁴) and the difference between axial and equatorial bond lengths (0.028 vs 0.055 Å experimentally⁶⁴). In the case of the unknown fluoroarsoranes AsH_nF_{5-n} ($n = 1-5$), our calculated structures serve as predictions, which are expected to be similar in quality to the results for the fluorophosphoranes and for AsF₅. The present theoretical structure of AsF₅ agrees with that from another ab initio study.²⁶

Considering the less stable isomers of the fluoroarsoranes and fluorophosphoranes, we note that the calculated equatorial bond distances increase and the axial ones decrease from isomers A to B and from B to C. Typical changes amount to 0.01-0.02 Å. The equatorial bonds are calculated to be shorter than axial bonds of the same kind in the less stable isomers, too, but sometimes these differences are much less pronounced (e.g., compare R_{eq} with R_{ax} in isomer B of AsHF₄ or r_{eq} with r_{ax} in isomer B of PH₂F₃). The structure of the activated complex of MH₄F ($M = \text{P}, \text{As}$) is characterized by similar bond lengths for the equatorial and axial hydrogen atoms (r_{eq} and r_{ax}), a large M-F distance, and large deviations of the bond angles from the values of an ideal trigonal bipyramid.

Table VI lists the unscaled theoretical harmonic frequencies ω_i , the scaled theoretical frequencies ν_i , and the calculated absolute

(48) Holmes, R. R.; Storey, R. N. *Inorg. Chem.* **1966**, *5*, 2146.
 (49) Treichel, P. M.; Goodrich, R. A.; Pierce, S. B. *J. Am. Chem. Soc.* **1967**, *89*, 2017.
 (50) Pierce, S. B.; Cornwell, C. D. *J. Chem. Phys.* **1968**, *48*, 2118.
 (51) Seel, F.; Velleman, K. *Z. Anorg. Allg. Chem.* **1971**, *385*, 123.

(52) Holmes, R. R.; Hora, C. J., Jr. *Inorg. Chem.* **1972**, *11*, 2506.
 (53) Hoffmann, R.; Howell, J. M.; Muetterties, E. L. *J. Am. Chem. Soc.* **1972**, *94*, 3047.
 (54) Keil, F.; Kutzelnigg, W. *J. Am. Chem. Soc.* **1975**, *97*, 3623.
 (55) Holmes, R. R. *J. Am. Chem. Soc.* **1978**, *100*, 433.
 (56) Strich, A. *Inorg. Chem.* **1978**, *17*, 942.
 (57) McDowell, R. S.; Streitwieser, A., Jr. *J. Am. Chem. Soc.* **1985**, *107*, 5849.
 (58) Deiters, J. A.; Holmes, R. R.; Holmes, J. M. *J. Am. Chem. Soc.* **1988**, *110*, 7672.
 (59) Beckers, H.; Breidung, J.; Bürger, H.; Kuna, R.; Rahner, A.; Schneider, W.; Thiel, W. *J. Chem. Phys.* **1990**, *93*, 4603.
 (60) Christen, D.; Kadel, J.; Liedtke, A.; Minkwitz, R.; Oberhammer, H. *J. Phys. Chem.* **1989**, *93*, 6672.
 (61) Downs, A. J.; McGrady, G. S.; Barnfield, E. A.; Rankin, D. W. H. *J. Chem. Soc., Dalton Trans.* **1989**, 545.
 (62) Kurimura H.; Yamamoto, S.; Egawa, T.; Kuchitsu, K. *J. Mol. Struct.* **1986**, *140*, 79.
 (63) Hehre, W. J.; Radom, L.; Schleyer, P. v. R.; Pople, J. A. *Ab Initio Molecular Orbital Theory*; Wiley: New York, 1986.
 (64) Clippard, F. B., Jr.; Bartell, L. S. *Inorg. Chem.* **1970**, *9*, 805.

Table V. Molecular Geometries^a of the Trigonal-Bipyramidal Isomers of the Fluoroarsoranes (M = As) and the Fluorophosphoranes (M = P)

molecule	isomer ^b	M	type ^c	r_{eq}	r_{ax}	R_{eq}	R_{ax}	$\alpha_{eq}, \beta_{eq}^d$	β_{ax}	γ_{eq}	γ_{ax}
MH ₅	C	As	T	1.509	1.584						
	C	P	T	1.407	1.470						
MH ₄ F	B	As	T	1.485	1.550		1.788	119.8			87.7
	B	P	T	1.389	1.443		1.651	120.0			89.3
	C ^e	As	T	1.507	1.518	1.757		103.3			82.6
	C ^e	P	T	1.404	1.418	1.617		103.1			84.6
MH ₃ F ₂	A	As	T	1.473			1.757				
	A	P	T	1.378			1.633				
	A	P	E ^f	1.394 (4)			1.6468 (2)				
	B	As	T	1.486	1.522	1.696	1.741	115.7	85.1	121.9	89.1
	B	P	T	1.387	1.418	1.572	1.618	115.8	87.4	122.1	89.8
	C ^g	As	T	1.506	1.503	1.712					
	C ^g	P	T	1.403	1.403	1.580					
	A	As	T	1.471		1.665	1.726		89.1	117.8	
MH ₂ F ₃	A	P	T	1.373		1.549	1.606		90.5	117.6	
	A	P	E ^h	1.375 (17)		1.539 (5)	1.618 (4)		91.9 (4)	117.1 (17)	
	A	P	E ⁱ	1.322 (11)		1.544 (4)	1.613 (2)		91.7 (2)	119.6 (44)	
	B ^g	As	T	1.475	1.488	1.681	1.712				
	B	P	T	1.383	1.397	1.561	1.592	123.7	88.4	118.1	89.9
	C	As	T			1.477	1.701				
	C	P	T			1.379	1.574				
	A	As	T	1.470		1.653	1.698			121.8	91.0
	A	P	T	1.369		1.538	1.585			122.1	89.5
	A	P	E ^h	1.363 (26)		1.539 (3)	1.596 (3)			122.8 (3)	88.8 (5)
MHF ₄	A	P	E ⁱ	1.324 (46)		1.537 (4)	1.591 (4)			123.0 (9)	87.8 (2)
	B	As	T		1.481	1.670	1.676	119.9	88.4		
	B	P	T		1.377	1.551	1.571	120.0	89.3		
	A	As	T			1.644	1.672				
	A	As	E ^j			1.656 (4)	1.711 (5)				
	A	P	T			1.531	1.566				
MF ₅	A	P	E ^k			1.529 (3)	1.576 (3)				

^a Bond lengths in angstroms; bond angles in degrees; equilibrium values, unless noted otherwise. For notation of bond lengths see text; the notation of the angles is the following: $\alpha_{eq} = H_{eq}MH_{eq}$; $\beta_{eq} = F_{eq}MH_{eq}$; $\beta_{ax} = F_{eq}MF_{ax}$; $\gamma_{eq} = H_{eq}MF_{ax}$; $\gamma_{ax} = H_{eq}MF_{ax}$ and $F_{eq}MH_{ax}$, respectively. ^b A, B, C with 2, 1, 0 axial fluorine atoms. ^c T = theoretical; E = experimental; uncertainty of last digit given in parentheses. ^d α_{eq} for MH₄F and MH₃F₂; β_{eq} otherwise. ^e Saddle point structure (see Table IV and text). ^f Reference 59; r_o structure. ^g The given data refer to optimized bond lengths, while the angles were taken from an ideal trigonal bipyramid; see text. ^h Reference 60; r_2 structure. ⁱ Reference 61; r_a structure. ^j Reference 64; r_g structure. ^k Reference 62.

infrared intensities A_i for the fluoroarsoranes (i.e., their most stable isomers), together with the available experimental data^{16-18,23,43} for AsF₅. The theoretical harmonic force fields for the arsoranes have been scaled with the use of our standard scale factors (see Table III). The vibrational spectrum of AsF₅ is well-known experimentally^{16-18,23,43} and can thus be used to check the accuracy of our theoretical results. Considering the As-F stretching modes first, we note that the degeneracy-weighted average value of the four corresponding scaled theoretical frequencies is quite close to the experimental value (763 vs 757 cm⁻¹ experimentally). Consistent with the errors in the calculated As-F distances (see above), both the equatorial and the axial As-F stretching frequencies are predicted somewhat too high (average errors of 5 and 6 cm⁻¹, respectively). The calculations reproduce the splittings between the antisymmetric and symmetric modes in both cases very well (equatorial, 76 vs 77 cm⁻¹; axial, 145 vs 143 cm⁻¹ experimentally), so that the absolute errors of the calculated As-F stretching frequencies fall between 5 and 7 cm⁻¹ (see Table VI). For the bending modes, the scaled theoretical frequencies are close to experimental values, the errors being in the range 7-10 cm⁻¹. The overall rms deviation between scaled theoretical and observed frequencies is 8 cm⁻¹. In our opinion, the transfer of scale factors from AsF₃ to AsF₅ is justified by these results, which indicate that the major differences between trivalent and pentavalent arsenic compounds can be described correctly at the chosen level of theory.

Turning to the infrared intensities of AsF₅, we note that the a_1' and e'' transitions are dipole-forbidden and have been observed only in the Raman spectrum.¹⁷ For the remaining five modes, the theoretical and experimental relative intensities are in good agreement (see Table VI). In particular, the calculation correctly predicts ν_3 and ν_5 to be the two strongest bands and ν_7 to be by far the weakest band.

Since the fluoroarsoranes AsH_nF_{5-n} ($n = 1-5$) are unknown molecules, the theoretical results in Table VI represent predictions of their vibrational spectra. The accuracy of the predicted As-F

stretching frequencies may be estimated from the results for AsF₅; these frequencies are probably too high by 5-10 cm⁻¹. The errors for the bending modes are normally believed to be about 20 cm⁻¹, according to our experience with the fluorophosphoranes² and AsF₅ (see above). The accuracy of the predicted As-H stretching frequencies is more difficult to estimate, because there are no experimental data for comparison. In this connection, it may be helpful to remember that the scaling procedure used in this work attempts to remove systematic errors in the calculations, which may be due to basis set incompleteness, the neglect of electron correlation, and the neglect of anharmonicity. This procedure is expected to be successful if the corresponding corrections are uniform for related molecules. Since the anharmonicity corrections for the P-H stretching frequencies have recently been found⁶⁵ to differ by about 20-50 cm⁻¹ in PH₃ and PH₂, one might expect an analogous situation for the As-H stretching frequencies. Therefore we cannot exclude errors of more than 20 cm⁻¹ in such cases, particularly for the axial As-H stretching modes, where correlation effects are supposed to be important.

The trends in the scaled theoretical frequencies (see Table VI) for the fluoroarsoranes are the same as those for the analogous phosphoranes.² The axial As-F stretching frequencies increase with increasing fluorine content, while the equatorial As-F stretching frequencies do not change very much; the As-H stretching frequencies are generally predicted to increase upon fluorine substitution. These trends in the scaled theoretical stretching frequencies are compatible with analogous trends in the corresponding bond lengths (see Table V). Turning to the bending frequencies, we see that their magnitude decreases from AsH₅ to AsF₅ mainly because of mass effects. The correlation diagrams for the stretching and bending frequencies of the

(65) Breidung, J.; Schneider, W.; Thiel, W.; Schaefer, H. F., III. *J. Mol. Spectrosc.* 1990, 140, 226.

Table VI. Vibrational Frequencies ω_i and ν_i (cm^{-1}) and Infrared Intensities A_i (km/mol) for the Fluoroarsoranes^a

molecule	mode	description ^b	calcd ^c		
			ω_i	ν_i	A_i
AsH ₃	a ₁ '	ν_1 s-str eq	2322	2096	0
		ν_2 s-str ax	1875	1692	0
	a ₂ ''	ν_3 a-str ax	1921	1733	944
		ν_4 a-def op	1131	1001	495
	e'	ν_5 d-str eq	2316	2090	278
		ν_6 d-bend ax	1169	1034	609
		ν_7 d-bend eq	597	528	13
		ν_8 d-def op	1411	1247	0
AsH ₄ F	a ₁	ν_1 s-str eq	2435	2198	4
		ν_2 AsH str ax	2152	1942	344
		ν_3 s-def op	1150	1022	180
		ν_4 AsF str ax	601	551	187
	e	ν_5 d-str eq	2469	2228	130
		ν_6 d-bend ax	1316	1165	95
		ν_7 d-bend eq	939	832	209
		ν_8 d-bend	585	520	41
AsH ₃ F ₂	a ₁ '	ν_1 s-str eq	2510	2266	0
		ν_2 s-str ax	633	581	0
	a ₂ ''	ν_3 a-def op	1230	1098	69
		ν_4 a-str ax	689	632	345
	e'	ν_5 d-str eq	2545	2297	94
		ν_6 d-bend eq	938	830	147
		ν_7 d-bend ax	268	239	69
		ν_8 d-def op	1128	1006	0
AsH ₂ F ₃	a ₁	ν_1 s-str eq	2543	2295	13
		ν_2 sciss eq	923	817	106
		ν_3 AsF str eq	825	757	57
	a ₂	ν_4 s-str ax	664	609	0
		ν_5 s-bend ax	272	244	26
		ν_6 AsH ₂ twist op	1154	1029	0
	b ₁	ν_7 a-str eq	2579	2328	49
		ν_8 AsH ₂ rock eq	676	603	88
		ν_9 a-bend ax	251	223	26
	b ₂	ν_{10} AsH ₂ def op	1229	1097	45
		ν_{11} a-str ax	748	686	310
		ν_{12} AsF def op	403	363	19
AsHF ₄	a ₁	ν_1 AsH str eq	2579	2327	21
		ν_2 s-str eq	826	757	53
		ν_3 s-str ax	690	634	2
	a ₂	ν_4 s-bend	408	365	89
		ν_5 s-bend	160	143	0
		ν_6 AsF ₂ twist op	407	366	0
	b ₁	ν_7 a-str eq	873	800	155
		ν_8 AsF ₂ rock eq	782	699	43
		ν_9 a-bend	271	244	22
	b ₂	ν_{10} AsH def op	1201	1072	16
		ν_{11} a-str ax	804	737	260
		ν_{12} AsF ₂ def op	426	383	47
AsF ₅ ^d	a ₁ '	ν_1 s-str eq	807	740	0
		ν_2 s-str ax	708	649	0
	a ₂ ''	ν_3 a-str ax	865	794	194
		ν_4 a-def op	438	393	84
	e'	ν_5 d-str eq	890	816	273
		ν_6 d-bend ax	406	365	146
	e''	ν_7 d-bend eq	156	140	1
		ν_8 d-def op	418	376	0

^aOnly the most stable trigonal-bipyramidal isomers are considered here. ^bBased on the calculated potential energy distributions. The equatorial and axial bending coordinates are usually mixed; if this mixing is almost even, the designation eq or ax is omitted for the corresponding bending modes. ^cFor scale factors see Table III; intensities refer to the scaled theoretical force fields. ^dObserved frequencies and relative intensities of AsF₅ (in standard notation): 734 Ra, 644 Ra, 787 vs, 400 s, 811 vs, 372 s, 132 w, 386 Ra.^{16-18,23,43}

fluoroarsoranes⁴⁶ are generally very similar to those for the fluorophosphoranes² and are therefore not reproduced here. The potential energy distributions characterizing the normal modes of the fluoroarsoranes are usually also very similar to those of the analogous phosphoranes.²

The scaled theoretical force fields for the fluoroarsoranes and the fluorophosphoranes are given in the supplementary material. Table VII lists the scaled theoretical symmetry force constants

Table VII. Scaled Theoretical and Empirical Force Fields for AsF₅ ($\text{mdyn}/\text{\AA}$)^a

	theor this work	empirical		
		ref 16 ^b	ref 22 ^b	ref 23 ^b
F_{11}	5.670	5.90 ± 0.105		
F_{12}	0.664	±0.5		
F_{22}	5.180	4.71 ± 0.105		
F_{33}	5.017	4.67 ± 0.37		
F_{34}	0.774	0-1.0		
F_{44}	1.567	1.86 ± 0.06		
F_{55}	5.557	5.204 ± 0.57	5.29 ± 0.25	5.38 ± 0.50
F_{56}	-0.048	±0.4	-0.24 ± 0.15	-0.13 ± 0.16
F_{57}	0.626	±0.4	0.01 ± 0.05	±1.0
F_{66}	0.337	1.224 ± 0.16	0.15 ± 0.05	0.64 ± 0.14
F_{67}	-0.374	0.000 ^c	0.00 ^c	0.94 ± 0.11
F_{77}	1.445	0.304 ± 0.04	2.21 ± 0.08	1.83 ± 0.31
F_{88}	1.239	1.457		

^aAngle-bending coordinates have been multiplied by a unit bond length of 1 Å. For scale factors see Table III. ^bSee text. ^cFixed.

Table VIII. Scaled Stretching Force Constants ($\text{mdyn}/\text{\AA}$) in Internal Coordinates^a

molecule	As-H ^b	As-H _{ax}	As-F ^b	As-F _{ax}
AsH ₃	2.639			
AsH ₂ F	2.590		4.124	
AsHF ₂	2.541		4.357	
AsF ₃			4.570	
AsH ₅	2.500	1.787		
AsH ₄ F	2.873	2.226		3.017
AsH ₃ F ₂	3.063			3.638
AsH ₂ F ₃	3.130		5.189	4.103
AsHF ₄	3.173		5.433	4.581
AsF ₅			5.594	5.098

^aFor scale factors see Table III. ^bEquatorial bonds in the case of the arsoranes.

for AsF₅ and compares them with the available empirical force fields,^{16,22,23} which reproduce the observed¹⁶ vibrational frequencies. Two empirical^{22,23} force fields that are limited to the e' block have also been fitted to experimental Coriolis data^{16,23} (f_5 and f_6) derived from band contour analyses. In one case,²³ two solutions have been determined for the e' block; in Table VII we quote the one preferred by the authors.²³ As can be seen from Table VII, most of the empirical^{16,22,23} force constants have large uncertainties, which are caused either by uncertainties in the Coriolis data²² or by the variations due to allowing a more or less plausible range of solutions for some interaction constants (F_{12} , F_{34} , F_{56} , and F_{57} in ref 16 and F_{57} in ref 23, respectively; see Table VII). The relation $F_{66} > F_{77}$ in the older empirical force field¹⁶ reflects the incorrect assignment of ν_6 and ν_7 to the in-plane and axial bending vibrations, respectively. Our force field for AsF₅ confirms the reverse assignment chosen in later empirical work.^{22,66} Because of the rather low quality of the empirical force fields^{16,22,23} for AsF₅, it does not seem worthwhile to compare them with the scaled theoretical results in full detail. A recent study²⁹ of the force fields of AsH₃ and AsF₃ has confirmed previous experience^{1,39} that deviations between scaled theoretical and well-determined empirical force constants are usually below 0.03 $\text{mdyn}/\text{\AA}$ and exceed 0.06 $\text{mdyn}/\text{\AA}$ only very rarely. Therefore we believe that, in a new empirical determination of the symmetry force constants for AsF₅, our scaled theoretical force constants may serve as realistic starting values or as constraints for the off-diagonal constants during the refinement.

Table VIII lists the scaled stretching force constants of the fluoroarsoranes in internal coordinates and compares them with those of the fluoroarsines. All trends in the stretching force constants upon fluorine substitution parallel those in the analogous phosphorus compounds,² and are again compatible with the trends

Table IX. Dipole Moments (D)

molecule	M = As			M = P		
	calcd	obsd	ref	calcd	obsd	ref
MH ₃	0.368	0.22 (2)	71	0.812	0.574	67
MH ₂ F	2.142			1.615		
MHF ₂	2.541			1.596	1.32 (1)	68
MF ₃	2.628	2.57 (2)	72	1.311	1.025 (9)	69, 70
		2.815 (25)	70			
MH ₄ F	2.434			1.801		
MH ₂ F ₃	2.095			1.451		
MHF ₄	2.209			1.483	1.32 (2)	50

Table X. Calculated Reaction Energies (kcal/mol)

reaction	M = As		M = P	
	ΔE_c^a	ΔE_o^a	ΔE_c^a	ΔE_o^a
Dissociations				
MH ₃ → MH ₃ + H ₂	-56.1	-60.0	-46.0	-50.9
MH ₄ F → MH ₃ + HF	-29.4	-32.0	-15.7	-19.4
MH ₃ F ₂ → MH ₂ F + HF	-2.8	-5.3	+13.6	+9.9
MH ₂ F ₃ → MHF ₂ + HF	-2.4	-4.6	+18.4	+14.9
MHF ₄ → MF ₃ + HF	-12.5	-14.5	+11.7	+8.5
Hydrogenations				
MH ₃ F ₂ + H ₂ → MH ₃ + 2 HF	-10.6	-10.9	+7.6	+6.1
MH ₂ F ₃ + 2H ₂ → MH ₃ + 3HF	-6.6	-4.0	+20.7	+22.1
MHF ₄ + 3H ₂ → MH ₃ + 4HF	-2.1	+3.8	+35.5	+40.3
MF ₃ + 4H ₂ → MH ₃ + 5HF	-0.4	+8.8	+48.0	+56.3 ^b
MF ₃ + 3H ₂ → MH ₃ + 3HF	+10.4	+18.3 ^c	+23.7	+31.8 ^d

^a ΔE_c without and ΔE_o with corrections for zero-point vibrational energies; these corrections have been calculated with the use of our scaled theoretical frequencies (see Tables II and VI and refs 1 and 2, respectively); zero-point energies for H₂ and HF have been calculated with the use of ω_e and $\omega_e x_e$ from ref 76. ^bExperimental: +58.1 kcal/mol.^{46,73} ^cExperimental: +10.2 kcal/mol.⁷³ ^dExperimental +27.1 kcal/mol.⁷³

in the bond lengths (see above). As expected, the stretching force constants usually increase with increasing fluorine substitution, with the exception of the As-H stretching force constants in the fluoroarsines, which decrease slightly (see Table VIII).

Table IX compares our calculated dipole moments for the fluoroarsines and fluoroarsoranes with those for the fluoro-phosphines and fluorophosphoranes, respectively. The available experimental^{50,67-72} data are also shown. In the case of the phosphorus compounds, the calculated dipole moments are always higher than the observed ones,^{50,67-70} by 0.16–0.29 D. Similar results had been obtained with the 6-31G** basis.¹ Therefore we do not expect the calculated dipole moments for the arsenic compounds to be more accurate than 0.3 D, although the results for AsH₃ and AsF₃ may suggest somewhat smaller errors. It is seen from Table IX that the dipole moments for the fluorinated arsines and arsoranes are predicted to be considerably higher than those for the analogous phosphorus compounds.

To provide some quantitative measure of the thermochemical stability, Table X lists the energies of reactions that convert the fluoroarsoranes to AsH_nF_{3-n} ($n = 0-3$) and HF (or H₂). This is accomplished by dissociation or hydrogenation reactions (see Table X). For the sake of comparison, the calculated data for the phosphoranes and for MF₃ (M = As, P) are also given. Although such reaction energies at the SCF level with medium-sized basis sets are sometimes not very reliable for hypervalent compounds,⁶³ the errors for the molecules studied should be reasonably small, since for the hydrogenation of PF₃ there is good agreement with the experimental value of 58.1 kcal/mol at $T = 0$ K (derived⁴⁶

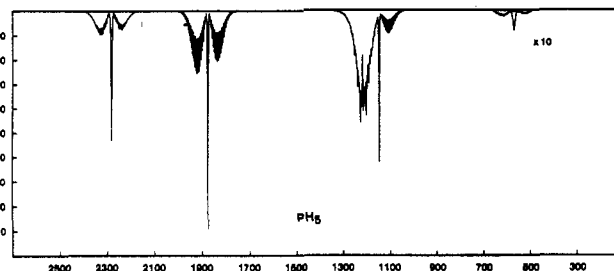
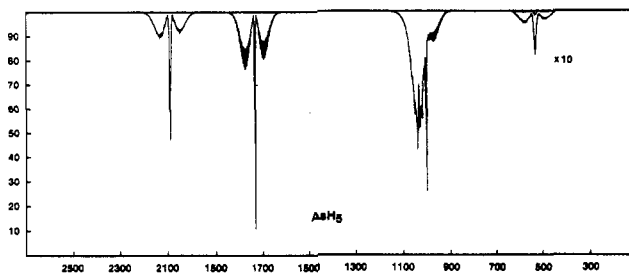


Figure 1. Predicted infrared spectra of MH₃ in the gas phase at 300 K: (top) M = As, $J'_{\max} = 35$, optical density $x = 0.08$ atm-cm; (bottom) M = P, $J'_{\max} = 30$; $x = 0.10$ atm-cm.

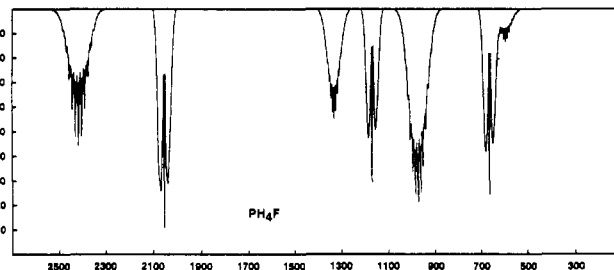
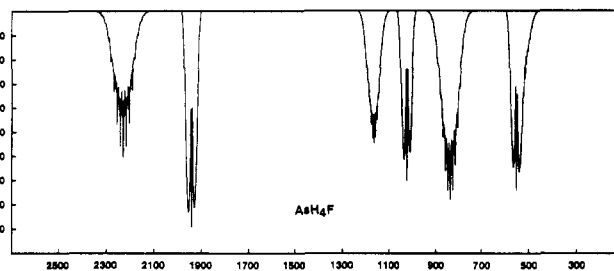


Figure 2. Predicted infrared spectra of MH₄F in the gas phase at 300 K: (top) M = As, $J'_{\max} = 65$; optical density $x = 0.09$ atm-cm; (bottom) M = P, $J'_{\max} = 55$; $x = 0.11$ atm-cm.

from standard enthalpies of formation⁷³ at $T = 298$ K) and since correlation corrections only amount to -4 kcal/mol (MP4 level)⁷⁴ and -0.4 kcal/mol (CI)²⁶ for PH₃ and AsH₃, respectively. In the case of the phosphoranes, the only exothermic dissociation reactions are associated with the unknown molecules PH₂ and PH₄F, while, for the arsoranes, all dissociations are predicted to be exothermic (see Table X). With regard to the hydrogenation reactions, the thermochemical stability increases successively with increasing fluorine content for both the phosphoranes and the arsoranes. The data in Table X show clearly that the fluoroarsoranes are much less stable thermodynamically than the analogous phosphoranes. It should be kept in mind, however, that all these molecules belong to local minima on their potential surfaces (see above). Therefore the kinetic stability is decisive for the existence of the as yet unknown fluoroarsoranes. Presently,

(67) Davies, P. B.; Neumann, R. M.; Wofsy, S. C.; Klemperer, W. *J. Chem. Phys.* **1971**, *55*, 3564.

(68) Kuczowski, R. L. *J. Am. Chem. Soc.* **1968**, *90*, 1705.

(69) Birnbaum, G. J. *J. Chem. Phys.* **1967**, *46*, 2455.

(70) Shulman, R. G.; Dailey, B. P.; Townes, C. H. *Phys. Rev.* **1950**, *78*, 145.

(71) McClellan, A. L. *Tables of Experimental Dipole Moments*; Freeman: San Francisco, London, 1963.

(72) Buckingham, A. D.; Raab, R. E. *J. Chem. Soc.* **1961**, 5511.

(73) Wagman, D. D.; Evans, W. H.; Parker, V. B.; Schumm, R. H.; Halow, I.; Bailey, S. M.; Churney, K. L.; Nuttall, R. L. *The NBS Tables of Chemical Thermodynamic Properties*; National Bureau of Standards: Washington, DC, 1982.

(74) Reed, A. E.; Schleyer, P. v. R. *Chem. Phys. Lett.* **1987**, *133*, 553.

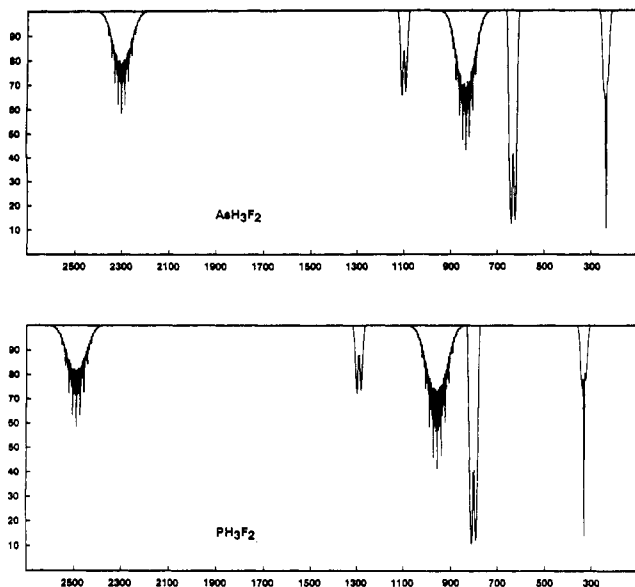


Figure 3. Predicted ($M = \text{As}$) and simulated ($M = \text{P}$) infrared spectra of MH_3F_2 in the gas phase at 300 K: (top) $M = \text{As}$, $J'_{\text{max}} = 90$; optical density $x = 0.03 \text{ atm}\cdot\text{cm}$; (bottom) $M = \text{P}$, $J'_{\text{max}} = 80$; $x = 0.03 \text{ atm}\cdot\text{cm}$.

no information on this subject is available for the arsoranes. In the case of the phosphoranes, the unknown molecule PH_3 has been calculated^{74,75} to be quite stable kinetically, with an activation energy of more than 30 kcal/mol for the loss of H_2 .

- (75) Kutzelnigg, W.; Wasilewski, J. *J. Am. Chem. Soc.* **1982**, *104*, 953.
 (76) Huber, K. P.; Herzberg, G. *Molecular Spectra and Molecular Structure*; Van Nostrand Reinhold: New York, 1979; Vol. 4 (Constants of Diatomic Molecules).

To conclude the present discussion of the fluoroarsoranes, Figures 1-3 present plots of the predicted infrared spectra of the symmetric-top molecules AsH_5 , AsH_4F , and AsH_3F_2 in the gas phase at 300 K and the corresponding theoretical spectra of PH_5 , PH_4F , and PH_3F_2 , respectively. The simulations of the spectra were carried out by using a modified version of the program KILO⁷⁷ and input data derived from scaled theoretical force fields⁴⁶ as described previously² (for vibrational frequencies and infrared intensities see Table VI). All rovibrational lines up to J'_{max} (see figure captions) and $K'_{\text{max}} = 20$ with intensities greater than a cutoff ($I_{\text{min}}/I_{\text{max}} < 0.002$) were generated and represented by Gaussian profiles of width $w = 3 \text{ cm}^{-1}$ to account for the spectral resolution. The resulting intensities were plotted as transmission spectra. The close relationship between the pairs of spectra for MH_5 , MH_4F , and MH_3F_2 ($M = \text{P}, \text{As}$) is obvious from Figures 1-3. In each case, the main difference is the red shift of the bands in the spectra of the arsenic compounds. The remarkable overall agreement between the observed^{51,59} and calculated^{2,59} infrared spectra of PH_3F_2 indicates that the spectra predicted for the other molecules are realistic and will hopefully facilitate their spectroscopic identification in the gas phase.

Acknowledgment. This work was supported by the Deutsche Forschungsgemeinschaft, the Fonds der Chemischen Industrie, and the Alfred-Krupp-Förderpreis. The calculations were carried out by using the CRAY X-MP/48 computer of HLRZ Jülich.

Supplementary Material Available: A discussion and listings of scaled theoretical force fields for the title compounds and the corresponding phosphorus compounds obtained with the use of effective core potentials (6 pages). Ordering information is given on any current masthead page.

- (77) Betrencourt-Stirnermann, C.; Graner, G.; Jennings, D. E.; Blass, W. E. *J. Mol. Spectrosc.* **1978**, *69*, 179.

Contribution from the Department of Chemistry,
 The Pennsylvania State University, University Park, Pennsylvania 16802

Complexation, Luminescence, and Energy Transfer of Ce^{3+} with a Series of Multidentate Amino Phosphonic Acids in Aqueous Solution

Steven T. Frey and William DeW. Horrocks, Jr.*

Received August 14, 1990

The luminescence of the Ce^{3+} ion in aqueous solution, which results from $d \rightarrow f$ transitions, is observed to be quenched by complexation with multidentate amino carboxylic acid ligands. However, the corresponding complexes containing phosphonic acid moieties show efficient room-temperature luminescence. Luminescence spectroscopy was used to characterize Ce^{3+} complexes with the following ligands: diethylenetriaminepentakis(methylphosphonic acid) (dtpp), ethylenediaminetetrakis(methylphosphonic acid) (edtp), hexamethylenediaminetetrakis(methylphosphonic acid) (hdtp), and nitrilotris(methylphosphonic acid) (ntp). Complex stoichiometries were determined by monitoring the emission intensity as a function of ligand concentration. The effect of pH on luminescence intensity was examined with quenching noted for higher pH values. Quantum yields of luminescence for each of the complexes were measured using $[\text{Ce}(\text{H}_2\text{O})_9]^{3+}$ as a standard. Energy transfer from Ce^{3+} to Eu^{3+} and to Tb^{3+} was observed to occur in binuclear complexes of dtpp, edtp, and hdtp. Although amino phosphonic acids are potential models for biological phosphate-containing molecules, ATP, tubercidin, and calf thymus DNA were all observed to quench Ce^{3+} luminescence.

Introduction

Cerium(III) luminescence has been observed for a variety of compounds and materials including phosphors,^{1,2} polymer films,^{3,4} cryptates,⁵ and, most recently, organometallic complexes.⁶⁻⁸

Although the luminescence of hydrated Ce^{3+} ions in aqueous solution has been studied quite thoroughly,⁹⁻¹² there have been no observations of Ce^{3+} luminescence in simple chelate complexes in this medium. In fact, all of the carboxylic acid containing ligands examined in this study and elsewhere^{13,14} quench Ce^{3+} ion

- (1) Blasse, G.; Brill, A. *Appl. Phys. Lett.* **1967**, *11*, 53.
 (2) Blasse, G.; Brill, A. *J. Chem. Phys.* **1967**, *47*, 5139.
 (3) Li, W.; Mishima, T.; Adachi, G.; Shiohara, J. *Inorg. Chim. Acta* **1986**, *121*, 93.
 (4) Li, W.; Mishima, T.; Adachi, G.; Shiohara, J. *Inorg. Chim. Acta* **1987**, *131*, 287.
 (5) Blasse, G.; Dirksen, G. *J. Inorg. Chim. Acta* **1987**, *133*, 167.
 (6) Rausch, M. D.; Moriarty, K. J.; Atwood, J. L.; Weeks, J. A.; Hunter, W. E.; Brittain, H. G. *Organometallics* **1986**, *5*, 1281.
 (7) Hazin, P. N.; Bruno, J. W.; Brittain, H. G. *Organometallics* **1987**, *6*, 913.

- (8) Hazin, P. N.; Lakshminarayan, C.; Brinen, L. S.; Knee, J. L.; Bruno, J. W.; Streib, W. E.; Folting, K. *Inorg. Chem.* **1988**, *27*, 1393.
 (9) Okada, K.; Kaizu, Y.; Kobayashi, H. *J. Chem. Phys.* **1981**, *75*, 1577.
 (10) Kaizu, Y.; Miyakawa, K.; Okada, K.; Kobayashi, H.; Sumitani, M.; Yoshihara, K. *J. Am. Chem. Soc.* **1985**, *107*, 2622.
 (11) Okada, K.; Kaizu, Y.; Kobayashi, H.; Tanaka, K.; Marumo, F. *Mol. Phys.* **1985**, *54*, 1293.
 (12) Miyakawa, K.; Kaizu, Y.; Kobayashi, H. *J. Chem. Soc., Faraday Trans. 1* **1988**, *84*, 1517.
 (13) Poluektov, N. S.; Kirilov, A. T. *Opt. Spektrosk.* **1967**, *23*, 762.
 (14) Boden, H. *Nature* **1969**, *222*, 161.